Towards Log-Polar Fixation for Mobile Robots – Analysis of Corner Tracking on the Log-Polar Camera

Albert Yeung Nick Barnes
Department of Computer Science and Software Engineering,
University of Melbourne, Victoria, 3010, AUSTRALIA
awy@cs.mu.oz.au *nmb@cs.mu.oz.au*

Abstract

Fixating on objects is fundamental to active vision tasks, such as reaching, navigation and docking. Most techniques generally have been designed for space-invariant cameras. This research proposes a new method for corner tracking to facilitate point fixation for a mobile robot using a foveated camera. When the target point is in the centre of the image, the fovea, its position can be accurately tracked at high resolution. At the same time, the periphery has a reduced pixel count thus reducing image processing computation compared to a uniform camera with the same field of view. If the target point suddenly moves into the periphery it still appears in the lower resolution part of the image and coarser control can bring it back into fovea.

Our experiment results demonstrate the stability of the proposed method and the performance of our implementation is adequate for real-time tracking applications.
Keywords: Log-Polar vision, fixation, Hough transforms, corner tracking, mobile robots.

1. Introduction

Active vision is an adaptive response to the demands of exploratory tasks. In [1], Ballard argues that fixation, the ability to acquire and to track a region of interest, is a basic operation in active vision. The ability to fixate reduces the complexity of higher-level vision problems by facilitating the use of coordinate frame of the target object. An example of this advantage can be seen in the docking problem. Given the ability to fixate on an environment point, docking with the corresponding object is simplified [2].

Most cameras are space-invariant, which means they have a uniform spatial resolution. Techniques for tracking and fixation for space-invariant cameras are well established (e.g. [6]). However, the extensive computation required in tracking algorithms means only a small field of view can be analysed at sustainable frame rates. On the contrary, a space-variant camera can analyse the same field of view at lower pixel count, thus enhancing processing speed without compromising resolution at the image centre. A log-polar camera achieves this with varying spatial resolution, maximal at the centre, reducing logarithmically towards the edge.

For log-polar cameras, methods have been developed for fixation based on colour [10], and templates [4]. However, target objects often cannot be discriminated simply by colour, while for manufactured objects, corners are often visible. In the case where a corner is visible, corner-based methods should be exploited for the speed increases that are possible through specialised algorithms. Corner based fixation can also be used to establish a precise correspondence between a fixated target and a corresponding object model, and thus facilitate knowledge-based interaction.

This research purports a method for corner fixation using a log-polar camera. An implementation of the technique is demonstrated and the results show that it could be applied to control a mobile robot or camera mount tracking a corner. This facilitates object centred coordinates for interaction with known objects. We also highlight some limitations of this of the present implementation that are being resolved in continuing research.

1.1. The Log-Polar Sensor

The log-polar sensor is an example of biological inspiration and has been applied in many areas of computer vision, such as pattern recognition [13], foveation [8], [3], and tracking [4], [9]. The log-polar sensor imitates the mapping from retina to visual cortex of primates [12]. In the retinal plane (Figure 1a), a point can be represented by Cartesian coordinates (x, y) or polar coordinates (r, ϕ), which are related by:

$$x = r\cos\phi, \quad y = r\sin\phi \tag{1}$$

The mapping between a polar plane (r, ϕ) (retinal plane) and a Cartesian plane (ξ, η) (log-polar cortical plane, Figure 1b), can be written as:

$$\xi = \ln\frac{r}{r_0}, \tag{2}$$

$$\eta = q\phi, \tag{3}$$

where r_0 is the radius of the innermost circle and $1/q$ is the minimum angular resolution of the log-polar layout.

A CMOS implementation of the log-polar sensor has been realised in [11] and is used in this research. This overcomes problems that may be experienced in a software implementation [5], such as foveal over-sampling and lack of interpolation in periphery.

2. Corner Tracking in Log-Polar Space

While tracking can be performed on many potential object geometries, corners are a common feature on manufactured objects. Corners are also good fixation points because the two intersecting edges, which define a corner, localise its position in two dimensions.

The two edges that form a corner exhibit a steady behaviour in log-polar space during movement. When the corner coincides with the foveal centre, the two edges align with radial lines in the image plane. These radial lines transform to straight lines in the log-polar image. As the corner moves off centre, the foveal part of the edge curves rapidly and retreats towards the periphery. The general slope of the edge increases as it moves away from centre. Figure 2 illustrates how the edges of the corner distort through movement.

It should be noted that the right-angled corner in one quadrant is sufficient for analysis purposes as differently angled corners only translate the edges along the η direction in log-polar space. Further, motion through the centre of the image and in different quadrants can be handled by symmetries. Nevertheless, there is a requirement for the lines that make up the corner to occupy a large proportion of the image, for shorter lines the following line model degenerates due to non-linearity.

2.1. Modelling Edge Distortion

Although it does distort as a curve, we fit a straight line to model the outer part of the edge. The slope of the fitted line varies monotonically with the degree of distortion. As we shall see in the results, this distortion varies with the distance of the corner from centre. Thus, the line parameters can be used to estimate the amount of off-centre movement. This estimation can then be used as a control feedback to correct the camera angle or robot position. This enables the platform to track corners.

To fit lines to edges in an array of pixels, a few image processing steps are required:

- Apply an edge detection mask, Sobel [7, p.339] in this case.
- Threshold the resultant gradient magnitude image at suitable level to bring out significant edges.
- Perform Hough transform technique to fit lines to edges [7, p.578].
- Locate peaks in Hough voting space.

Smoothing, noise removal or other filters can be applied if necessary.

Standard implementations of edge detection and Hough transform are applied. The (ρ, θ) line parameterisation (Figure 3) handles lines of any orientation:

$$\rho = x\cos\theta + y\sin\theta \tag{4}$$

As we are using a straight line to model a curve, many lines exhibit a partial fit. However, we want to model the angle at the outer edge of the image to measure distortion thus we seek the outermost, and most horizontal part of the curve. We introduce two biases in Hough voting to facilitate this: horizontal line bias; and, *x*-bias on edge pixels that are more than a certain distance away from centre. In our implementation, the horizontal bias was one vote per edge pixel and the *x*-bias of one vote for edge pixels in the right quarter of the image (i.e. for $x > 60$, where image width is 76 pixels). This improved experimental performance for corners in the periphery.

2.2. Log-polar image discontinuity

In a true log-polar image, the η parameter is continuous across 0° and 360°. However, in order to represent such image in a conventional 2-D format, an arbitrary split is introduced. Hough space must be remapped to allow for this discontinuity.

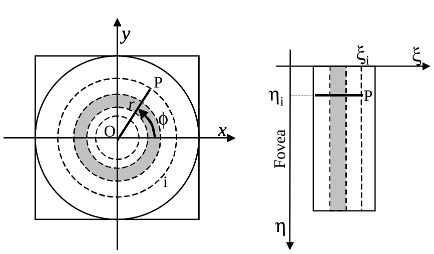

(a) (b)

Figure 1. Log-Polar Mapping. An annulus in the image plane (a) maps to a vertical strip in the remapped Cartesian plane (b).

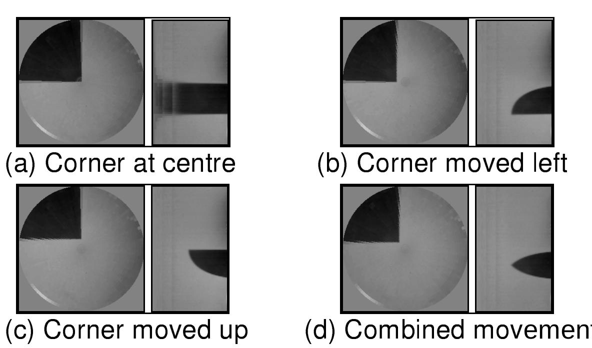

(a) Corner at centre (b) Corner moved left

(c) Corner moved up (d) Combined movement

Figure 2. Log-polar (left) and Cartesian remapped (right) images of a corner in 4 positions.

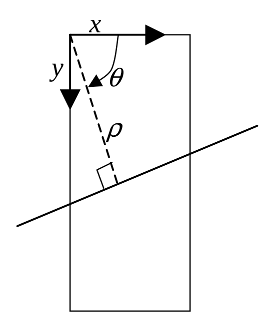

Figure 3. $\rho\theta$ Line Parameterisation.

3. Experiment Setup

Figure 4 shows the scaled-down A4 size static target used. The target was fixed on a wall, while the camera was mounted on a camera stand with some degree of freedom. The motion of the corner is defined relative to the captured image. Three type of motion were tested: leftwards - by panning camera clockwise; upwards - by lowering the camera; and, combined. A natural scene within the laboratory is also used to verify against a real world image.

4. Results

After Hough voting is performed, two peaks in the voting space are located to give the line parameters of two lines of best fit. They are drawn as white lines for illustration in Figure 6. As the corner moves away from fovea, a steady increase in the slope of line can be observed on the distorted edges. This is clearly shown in the first three columns of images in Figure 6a-c.

As the corner moves towards the edge of image, some images in the last column of Figure 6a-c show more than two lines. This is due to limited voting resolution when only a small part of the corner is visible, leading to a small number of edge pixels to vote on. This increases the likelihood of peaks having equal votes. To maintain stability in a hardware implementation, different control gains may be required to move the target back towards centre of image. After which the normal fine control can again be applied.

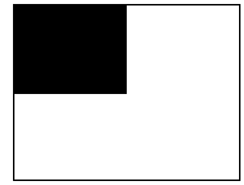

Figure 4. Artificial corner target.

Figure 7 shows the plots of line parameters versus corner off-centre distance. Note that there are two traces for each parameter plotted. Each trace represents one of the corner edges. There is a potential discontinuity when the detected line crosses the origin for line parameterisation. However, this can be eliminated by allowing ρ to become negative, interpreting it as an extension to the opposite direction of θ (Figure 5).

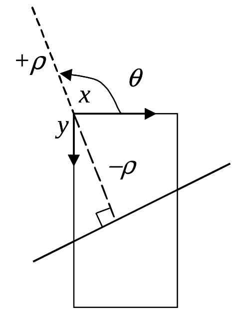

Figure 5. $-\rho$, $\theta - 180$ Line Parameterisation.

4.1. Natural Scenes

A natural scene (Figure 8) is also used to test robustness of the proposed method. Most of the additional complexities are shown to be well handled by the method: general visual clutter is filtered out in edge detection and Hough voting processes; and, shortened corners behave in the same manner as full corners. However, in cases where more than one corner is detected, the issue of deciding which corner to track is not handled by the method. A good solution would use additional image features to find the correct corner to track, which could be

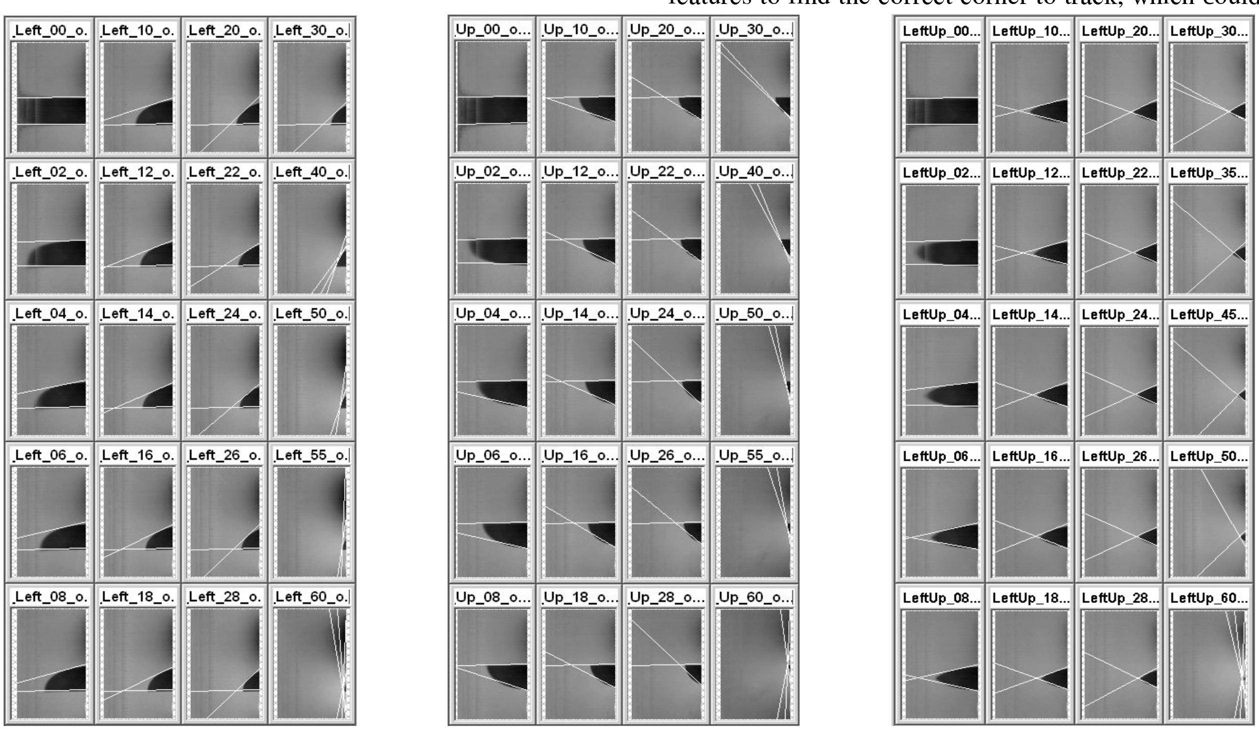

(a) (b) (c)

Figure 6. Series of log-polar images on Cartesian plane captured from the camera for corner movements at various distance of leftward, upward and combined leftward and upward respectively.

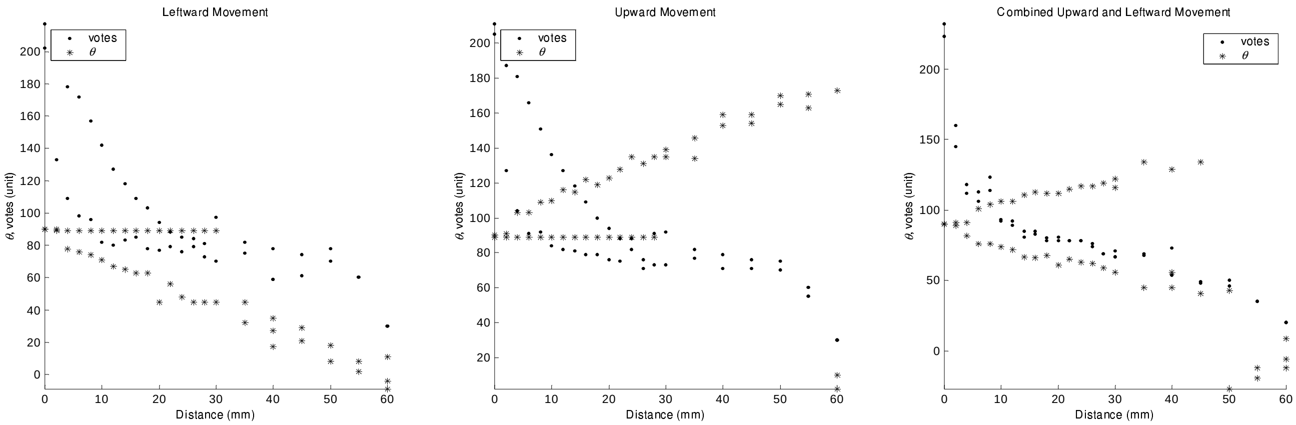

(a) **(b)** **(c)**

Figure 7. Plot of fitted line parameters versus corner distance from centre.

combined with this method. A possible approach would be to track the corner closest to the image centre, but this was not explored further in this paper.

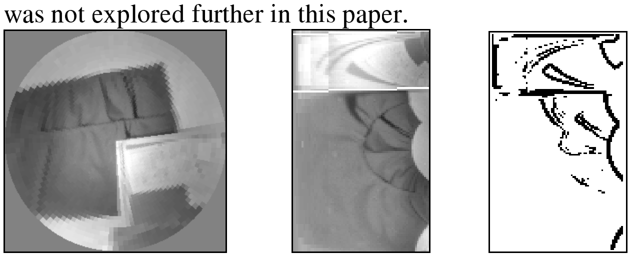

Figure 8. A natural scene, in log-polar space and the corresponding edge map.

5. Conclusion and Further Work

We have developed and demonstrated a method for corner tracking for log-polar cameras. Our algorithm runs at 10 frames/sec, which is adequate for real-time processing and would improve with optimisation. This method will facilitate high-speed log-polar corner fixation. We are now implementing the method on a pan-tilt platform mounted on a mobile robot. We are also applying a more sophisticated corner model to overcome instabilities with short lines and multiple corners.

6. Acknowledgement

The authors would to thank and G. Sandini for the use of the log-polar camera.

7. References

[1] Ballard DH. Animate Vision. In *Artificial Intelligence*, vol.48, no.1, Feb. 1991, pp.57-86. Netherlands.

[2] Barnes N, Sandini G. Direction Control for an Active Docking Behaviour Based on the Rotational Component of Log-Polar Optic Flow. In *Proc. Sixth European Conference on Computer Vision*, Part II, June/July 2000. Springer 2000, pp.167-181. Dublin, Ireland.

[3] Baron T, Levine MD, Yeshurun Y. Exploring with a foveated robot eye system. In *Proc. of the 12th IAPR Intl. Conf. on Pattern Recognition*, IEEE Comput. Soc. Press. Part vol.3, 1994, pp.377-380 vol.3. CA, USA.

[4] Bernardino A, Santos-Victor J. Binocular tracking: integrating perception and control. In *IEEE Transactions on Robotics & Automation*, vol.15, no.6, Dec. 1999, pp.1080-1094. Publisher: IEEE, USA.

[5] Capurro C, Panerai F, Sandini G. Dynamic vergence using log-polar images. In *Intl. Journal of Computer Vision*, vol.24, no.1, 1997, pp.79-94. Publisher: Kluwer Academic Publishers, Netherlands.

[6] Hager GD. Belhumeur PN. Efficient region tracking with parametric models of geometry and illumination. In *IEEE Transactions on Pattern Analysis & Machine Intelligence*, vol.20, no.10, 1998, pp.1025-39. USA.

[7] Haralick RM, Shapiro LG. Computer and Robot Vision. Addison-Wesley Publishing Company, Inc. USA.

[8] Lim FL, West GAW, Venkatesh S. Use of log polar space for foveation and feature recognition. In *IEE Proc.: Vision, Image & Signal Processing*, vol.144, no.6, Dec. 1997, pp.323-331. Publisher: IEE, UK.

[9] Odo S, Hoshino K. Real time object tracking based on retino-cortical mapping. In *Proc. of the 9th IEEE Intl. Workshop on Robot and Human Interactive Communication*, IEEE RO-MAN. 2000, pp.47-51. Piscataway, NJ, USA.

[10] Panerai F, and Metta G, Sandini G Towards Visuo-inertial stabilisation in space variant binocular systems. Robotics and Autonomous Systems, vol.30, no. 1-2, 2000, pp. 195-214.

[11] Questa P. Sandini G. Time to contact computation with a space-variant retina-like C-mos sensor. In *Proc. of 1996 IEEE/RSJ Intl. Conf. on Intelligent Robots and Systems*, IEEE. Part vol.3, 1996, pp.1622-9 vol.3. NY, USA.

[12] Schwartz EL. Spatial mapping in the primate sensory projection: Analytic structure and relevance to perception. In *Biological Cybernetics*, vol.25, no.4, 1977, pp.181-94. West Germany.

[13] Wilson JC, Hodgson RM. A pattern recognition system based on models of aspects of the human visual system. In *Intl. Conf. on Image Processing & Applications*. no.354. IEE. 1992, pp.258-261. London, UK.